57p.

PARALLEL INVERTER AND CONVERTER OPERATION AND IMPROVEMENTS IN TRANSFORMERS

NASA CONTRACT ~~NO.~~ NAS 3-2792

Second Quarterly Report, ~~For The Period~~
September 28, 1963 to December 27, 1963

PREPARED FOR THE NATIONAL AERONAUTICS AND SPACE ADMINISTRATION

BY:
G. W. Ernsberger and
H. R. Howell

1963 57p mfa

Westinghouse Electric Corporation
AEROSPACE ELECTRICAL DIVISION
LIMA, OHIO

NASA-CR-54012

PARALLEL INVERTER AND CONVERTER OPERATION AND IMPROVEMENTS IN TRANSFORMERS

CONTRACT NO. NAS 3-2792

Second Quarterly Report For The Period
September 28, 1963 to December 27, 1963

PREPARED FOR THE NATIONAL AERONAUTICS AND SPACE ADMINISTRATION

BY:
G. W. Ernsberger
H. R. Howell

Technical Management, NASA-Lewis Research Center
Auxiliary Power Generation Office, Francis Gourash

Westinghouse Electric Corporation
AEROSPACE ELECTRICAL DIVISION
LIMA, OHIO

TABLE OF CONTENTS

LIST OF FIGURES

LIST OF TABLES

SUMMARY

17760

A on Copy.

The technical analysis and design for this program were completed during the first quarter of the contract period. This work was described in the first quarterly report. Fabrication of two static inverter/converter test-models was started and about 60% completed during the second quarter. Transformer laminations were punched from Cubex Steel for the static-inverter output-transformer test-model. A test procedure was designed and written for laboratory evaluation of the test-models. It is expected that tests to be completed during the third quarter will demonstrate the feasibility and advantages of operating static inverters or converters in parallel as contrasted to the simple use of redundant units. They will also confirm the anticipated improvement in static inverter transformer efficiency with use of field-annealed doubly-oriented silicon-steel.

AUTHOR

I. INTRODUCTION

The purposes of this contract are (1) to develop means for parallel operation of static inverters and converters, and (2) to evaluate the use of Cubex steel as a means of increasing the efficiency and/or the power-to-weight ratio of static inverters.

The analytical work and the design work were completed during the first quarterly reporting period as described in the first quarterly report. This quarter's objectives were to begin building electrical test-models, and to prepare a test program for laboratory evaluation of the concepts developed during the analytical and design stages of this contract. This report describes the progress in these areas.

During the third quarter, the test-models and the laboratory evaluation will be completed. A qualitative reliability and weight analysis will show why and when it is advantageous to operate static inverters or converters in parallel.

II. FABRICATION OF STATIC INVERTER OUTPUT TRANSFORMER UTILIZING FIELD-ANNEALED DOUBLY-ORIENTED SILICON-STEEL

The Cubex-steel transformer-core laminations were fabricated and sent to Westinghouse Research and Development Center to be field-annealed. The coil forms, wire, and other components have been provided. The output transformer will be assembled with the field-annealed Cubex-steel punchings next quarter.

Current data on Cubex-magnetic material are included in Appendix I. This IEEE District Paper, "Cubex Magnetic Cores for Aerospace Electrical Equipment", was presented as an unprinted District IEEE paper in Toledo May 8, 1963. The written form of this paper appears in Appendix I through the courtesy of the author, Dr. A. C. Beiler, Chief Scientist, Westinghouse Aerospace Electrical Division, Lima, Ohio. This paper, mentioned in the first quarterly report, presents an informative description of Cubex-steel, its magnetic characteristics, and the effect field-annealing has on these characteristics. Most of the data presented are based on round cores, but the data give a good early indication of the material's capabilities.

III. FABRICATION OF STATIC INVERTER/CONVERTER MODELS FOR PARALLELING EVALUATION

Assembly of the inverter/converter test-models is now 60% complete with about 95% of the bought-outside parts received. Because of problems in procuring timely delivery of cores for ten different magnetic components, complete assembly of the inverter/converter test-models will be delayed until the middle of next quarter.

IV. TEST PROGRAM FOR TRANSFORMER AND PARALLELING EVALUATION

A test procedure was written to direct the laboratory evaluation of the Cubex-steel transformer and the paralleling of the two inverter/converter electrical models. The test procedure is Appendix II.

A. Parallel Inverter Evaluation.

The electrical models will first be operated as isolated static inverters to measure the load-division-circuit gain. The accuracy of this circuit design will be checked by supplying rated load current at 0.5 lagging power factor from one inverter model. When the load-division current-transformer secondary is not shorted, the inverter output voltage is designed to decrease from a nominal value of 115 volts to approximately 67.5 volts. This characteristic will be checked on both inverter models.

Next, the operation of the frequency-locking circuits will be checked. When both inverter models are energized, only one of the two tuning-fork frequency references should start and will determine the output frequency of both inverter models. This frequency-locking circuit is designed to select automatically, one of two or more tuning-fork oscillators in a parallel inverter system, and use the selected oscillator to control the frequency of all the paralleled inverters. In some parallel system applications, it may be preferable to eliminate this frequency-locking circuit by using only one frequency reference for the entire system.

The operation of the phase-lock circuits will then be tested. This interconnection of inverters is designed to assure that both inverters produce three-phase output voltages with corresponding phase voltages in-phase with each other. For example, with the phase-lock circuits operating properly, phase A output voltage of inverter I will be in phase with phase A output voltage of inverter II. This is a condition which must be met before connecting the inverter output terminals in parallel.

The load-division current-transformer secondary terminals, X1 and X2, will be short circuited during normal isolated-inverter operation. This allows an electrical load to be connected to the isolated-inverter without the output voltage drooping because of the load-division-circuit gain. When the inverter-model output terminals are connected in parallel, the load-division current-transformer secondaries are connected in a series loop as shown in Figure 9 of Appendix II. These current-transformer interconnections will be made automatically with auxiliary contacts on the paralleling circuit breaker. During parallel operation, a variety of loads will be used from 0 to 125% rated load with power factors from 0.9 leading to 0.75 lagging. Ammeters and wattmeters will be used to determine how well the load is shared between inverters under

steady-state conditions. A recording oscillograph will be used to record load sharing characteristics during paralleling transients and load transients.

B. Parallel Converter Evaluation.

Each static inverter model will be used as a static converter model by rectifying the delta connected inverter output voltage with a three-phase full-wave rectifier. This rectifier is included in the model and the necessary terminal board connections for single converter operation are shown in Figure 10 of Appendix II. These interconnections result in a converter with a rated output of 153.5 volts, 4.88 amperes, d-c.

With rated load applied to an isolated-converter model, the d-c load division circuit will be adjusted so that 20 volts, d-c, is measured between terminals Y1 and Y2. This adjustment will be repeated for the second converter.

When the two converter output terminals are connected in parallel, the Y1 and Y2 terminals of converter I must be connected to the Y1 and Y2 terminals respectively of converter II shown on Figure 11 of Appendix II. This will be accomplished automatically with auxiliary contacts on the paralleling circuit breaker. (The operation of this d-c load division circuit is described in the first quarterly report and is adapted from methods used to operate regulated transformer-rectifiers or regulated d-c generators in parallel.) Ammeters and wattmeters will be used to record the steady-state load division between the paralleled converters. Loads from 0 to 125% will be applied; a recording oscillograph will be used to record load current division during all paralleling and load transients.

C. Transformer Evaluation.

The effect of using Cubex-steel in the inverter output transformer will be evaluated by measuring transformer temperature rise and inverter efficiency. These measurements will first be made with the singly-oriented, silicon-iron core in the inverter output transformer. This output transformer will then be replaced with an identical transformer having a Cubex-steel core. Inverter efficiency and output transformer temperature rise will again be measured at both zero and full load. These measurements will illustrate the improved inverter efficiency caused only by changing the output transformer core material. This reduction in losses can be traded for reduced transformer weight. This would improve the power-to-weight ratio of the inverter without affecting efficiency. These trade-off possibilities will be calculated for the final report.

V. PLANS FOR FUTURE WORK

The two inverter/converter electrical models and static-inverter output transformer model will be completed during the first half of next quarter. These electrical models will be evaluated during the last half of next quarter in accordance with the test procedure in Appendix II. The evaluation is to be completed by the end of the third quarter.

A qualitative description of the factors contributing to increased system reliability at reduced weight, which result from paralleling inverters, will be prepared for the final report.

VI. CONCLUSIONS

Implementation of the test procedure in Appendix II will adequately demonstrate that successful paralleling of static inverters and converters has been achieved. This test procedure will demonstrate the load division capabilities of the proposed paralleling methods under both steady-state and transient conditions. This test will also illustrate the improved inverter efficiency made possible through the use of doubly-oriented field-annealed silicon-steel.

APPENDIX I

CUBEX MAGNETIC CORES FOR AEROSPACE ELECTRICAL EQUIPMENT

District Paper

I·E·E·E

CUBEX MAGNETIC CORES FOR AEROSPACE ELECTRICAL EQUIPMENT

A. C. Beiler
Member IEEE
Westinghouse Electric Corp.
Lima, Ohio

Presented May 8, 1963 at the session on Aerospace of the East Central and Allegheny-Ohio Valley District Meeting in Toledo, Ohio

Paper No. DP
63-797

CUBEX MAGNETIC CORES FOR AEROSPACE ELECTRICAL EQUIPMENT

A. C. Beiler

Summary. Data are presented on magnetic cores wound from newly developed 0.002" thick cube texture oriented Cubex silicon-iron tape. The cores are characterized by high permeability: 1900 at 10 oersteds; low coercive force: 0.2 oersted after a tip magnetizing force of 10 oersteds; and low core loss: 5.5 watts per pound at 15 kilogausses and 400 cycles per second. Magnetic field annealing generates even better properties.

INTRODUCTION

Those present at this session on Aerospace surely are aware of the importance of the use of high quality materials in aerospace electrical equipment. All one needs to do to impress himself with the necessity of high performance and extreme reliability is to mentally place himself in a space voyaging machine as an astronaut. The personal anxiety will make the point clear. Even if one takes a less personal approach and considers only the instrumented scientific data gathering space programs, the enormous cost of a space mission demands that the mission be successful. As taxpayers we must insist that reliable high quality apparatus be used. Such equipment requires the best in design andthe maximum performance of materials.

The needs of the space programs and the continuing domestic and military aircraft programs can only be met by continual improvements in equipment. The origins of these improvements come from three closely interrelated and interdependent sources:

1. The discovery of new scientific principles
2. The creation of new designs
3. The research that leads to new materials

Consequently it is in the national interest to continue this search for new principles, for better designs and for vastly improved new materials.

The first source of improvement, discovery of new principles, is a relatively rare occurrence and even when it happens it may have to wait for its realization until the other two are abreast of it. The opportunity to create a new design is often, but not always, dependent upon the existence of a new superior material. Many times the availability of a new material and an appreciation of its characteristics suggest a new device or a new way to accomplish the purposes of its less elegant or more cumbersome predecessor.

The capacitor offers a good example of this. The principles of its operation have been known for many years and are unchanged, but almost the only relationship a modern capacitor bears to its forebears is the operating principle. Much improved materials have permitted modifications in design that have brought us a vastly improved capacitor when compared to the earliest ones.

The entire history of industrial development is studded with similar cases. Perhaps (though admitting a personal bias) this has been most true of the electrical industry. Now the industry is being asked not only to extend its steady growth of improvements, but to accelerate the rate of improvement of equipment and to extend these improvements to extreme environmental conditions. Thus, when a new material with much improved properties comes on the scene, it is

important to know its characteristics well and to make sure that those who may have occasion to use it in their work have the opportunity to hear about it publicly.

Consequently it is both a duty and a pleasure for the writer to present information on a new magnetic material and a new magnetic core which may have profound effects on design of equipment, in which many of you participate.

The new material is 0.002" tape of doubly-oriented silicon-iron CUBEX alloy. Cores wound from this material have high magnetic permeabilities at high inductions, low coercive force and low total core loss over a range of frequencies. Typically the material has a permeability of 1900 at a magnetizing force of 10 oersteds, a coercive force of 0.2 oersteds measured from a tip magnetizing force of 10 oersteds and a 400 cycle core loss at 15 kilogausses of 5.5 watts per pound. Even these good characteristics can be improved by subjecting the core to a magnetic field during is annealing treatment.

HISTORY OF ORIENTATION DEVELOPMENT

Observation of Crystal Anisotropy.

It is both interesting and provides a better technical understanding of this material to review briefly the scientific and technical growth which lead up to cube texture. Such a review shows that the cube texture in silicon-iron has been a"long sought-for" development. Its probable technical advantages have been surmised by magneticians for many years.

The development of cube texture probably had its origin in the early studies of the properties of crystals. While studying crystals from a melt containing 1.6 per cent silicon K. Beck (1) observed

crystal anisotropy in 1918. Beginning about 1925 the literature contains reports of numerous investigators who steadily improved the data by refining the method of making more perfect stress-free crystals and by refining measurements techniques. With this refinement of accuracy in observations more precise evaluation of the constants in the relations for crystal anisotropy energy was possible.

In 1937 H. J. Williams (2) published measurements of the magnetization curves for the three principle directions of a single crystal of 3.8 per cent silicon iron (see Figure 1), which are in excellent agreement with magnetization curves calculated on the basis of anisotropy energy. From this figure it is clear that the easy direction of magnetization is the [001] direction or any cube edge. The intermediate direction is [011] or the cube face diagonal and the most difficult direction is the [111] direction or body diagonal of the cube. Schlectweg (3) disclosed a method for calculating the magnetization curve for any other orientation when the three basic curves of Figure 1 are known. Later R. M. Bozorth (4) described a graphical method for accomplishing the same thing.

Technical Motivation for Searching for a Method of Crystal Alignment

From the figure it is clear that the permeability is a maximum in the [001] direction. Further, since all the curves eventually reach the same saturation magnetic induction, the smallest hysteresis loop attainable will be that for the [001] direction. Since the differences between the magnetization curves for the three principle directions are so gross, it is clear that a magnetic circuit in which the [001] direction is lined up with the magnetic flux path at all points should have very high permeability and the lowest possible

total core loss, provided of course, that the crystals are free to a high degree from structural defects and from stress. In commercial polycrystalline material these latter restrictions are very difficult to meet. But for many years the most difficult part of the problem was to find a way to prepare magnetic sheet with any kind of controlled crystal orientation.

Most magnetic materials having cubic crystal structure are characterized by a random crystal structure where there is no apparent connection between the final average crystal structure of the sheet and any processing factors. This structure has been compared to a thoroughly shaken bag of blocks. In Figure 2 the arrangement of cubes marked "random" is an effort to portray graphically the random orientation of the iron crystals with respect to the length and width of a steel sheet (represented by the black strip) which is most common among the less sophisticated magnetic materials. Clearly, this structure eliminates any possibility of aligning an applied magnetizing force with all the cube edges. Thus one is forced to accept a mixture of the three principle magnetization curves as the magnetization curve for unoriented magnetic materials.

Discovery of Cube-onEdge Orientation and Its Limitations

This was the situation when Goss (5) disclosed processes of combining cold reduction and annealing which produced material of superior magnetic properties when measured parallel to the rolling direction of the material. His processes produced the structure illustrated in the central example of Figure 2 and described in 1935 by Bozorth (6). This structure is commonly called the "cube-on'edge", Goss texture or singly oriented material. The cube edges, [001] directions, are

lined up parallel to the rolling direction of the strip. Thus, in applications where it is possible to use a flux direction in the steel parallel to the rolling direction, one might ultimately expect to obtain properties similar to or approaching the properties of a single crystal in the [001] direction.

The relation of material properties to perfection of crystal alignment was realized very early. Considerable effort was applied by Goss himself, by Frey and Bitter (7), by Cole and Davidson (8) and by Carpenter (9) during the next few years to produce a more perfect crystal structure while applying processes which, though novel, were still compatible with steel mill practice. Eventually this led to availability of the cube-on-edge steel in the market place and it became a particularly significant factor in the transformer industry.

Constant attention by the producers to a mass of fine detail in terms of processing variables and material purity have continued to improve the electrical efficiency of this material to the extent that it is the most prominent single type of material in the high quality electrical industry today. The same type of attention to built-in quality promises to improve it in the future and similar attention to design and manufacture of apparatus from it promises still higher efficiency and lower apparatus weight in the future.

An examination of Figure 2 will disclose a limitation in the use of cube-on-edge material for certain applications where magnetic flux paths may have to go around corners or lie in different directions with respect to the rolling direction of the sheet. Although four edges of each cube are lined up with the rolling direction in the

cube-on-edge structure, the fact that the cube is standing on edge with respect to the plane of the sheet causes the (110) plane to lie in the plane of the sheet. If one applies a magnetizing force transverse to the rolling direction, it is in the [011] or face diagonal direction, which, from Figure 1, has intermediate ease of magnetization, but is considerably inferior to the [001] or cube-edge direction. If one considers other possible directions in the plane of a cube-on-edge sheet it will be seen that at 55 degrees away from the rolling direction the body diagonal or [111] direction would be effective. Magnetically this is the worst possible direction.

Discovery of Cube-on-Face Orientation, or Cube Texture

Now consider the upper example of Figure 2, the cube texture. Suppose one were able to control the structure of the alloy in such a way that the cube face could be made to lie in the plane of the sheet. Then there would be cube edges in the plane of the sheet and at right angles to each other and the worst condition to be found in the plane of the sheet would be at 45 degrees to the cube edges or in the cube face diagonal [011] direction. By reference to Figure 1 this can be seen to be the intermediate direction magnetically, and the [111] direction does not occur at all. Such material would be the cube face structure, but this does not imply that all cubes having a face in the plane of the sheet would necessarily be similar in alignment of edges. Still better would be the case where all cube face crystals are so aligned that all cube edges have the same relationship to the edges of the sheet. In particular, probably the most advantage could be taken of this texture if the two principle

directions of cube edges were parallel and transverse to the rolling direction of the sheet. This is what is meant by cube texture.

Like the cube-on-edge texture the probable value of the cube texture was recognized early and many laboratories worked for many years in an effort to learn how to cooperate with nature's forces so as to produce such a texture in silicon steel. As long ago as 1935 Sixtus (10) found a component of orientation which he identified as (100) [001] in silicon iron. The balance of the orientation in his material is principally the Goss (110) [001] texture. Bozorth, Williams and Morris (11) found evidence of cube texture in 3.5 percent aluminum iron alloys about 5 years later. Samples of their material showed equivalent permeability parallel and transverse to the rolling direction.

The first report of cube texture occupying more than 90 percent of the volume of a body centered cubic material was the result of work by Assmus (12, 13) and a team of co-workers, Detert, Ganz, Boll, Pfeifer, and Ibe at the Vacuumschmelze Laboratory in Hanau, Germany, using a method of secondary recrystallation in 3 percent silicon-iron.

In support of their findings they presented etch-pit patterns, x-ray pole figures, torque magnetometer curves and magnetization curves. The permeability of the 0.0016 inch 3.5 percent silicon-iron alloy tape was equal in the rolling direction and cross-wise to the rolling direction, and at high inductions the values were equivalent to the best commercially available cube-on-edge material of heavier gauge.

While it is really beyond the scope of this work to trace in

detail the metallurgical development history of this material in subsequent years, a number of references are included so that the reader interested in obtaining further information on this aspect of the cube texture material may find the pertinent references more easily. The problem was approached vigorously in several laboratories, as can be seen from the literature. At the General Electric Research Laboratory a team consisting of Hibbard, Walter, May, Turnbull, Pry and Dunn did a considerable amount of investigation on the characteristics of the texture and its origin. (see references 16, 17, 18, 19, 20, 27, 28, 29). At the Vacuumschmelze Laboratory, where the cube texture was first announced, efforts continued on the fundamental physics of the properties, vacuum annealing and other problems. There the team consisted of Assmus, Detert, Thomas, Ganz, Baer, Brenner and others. (see references 12, 13, 15, 22, 23, 25). At the ARMCO Steel Corporation Research Laboratories, D. Kohler (26) and others studied the effect of annealing atmosphere conditions and problems related to its manufacture. At the Westinghouse Research Laboratories still another team was working on various aspects of the problem. This group consisted principally of Wiener, Albert, Trapp, Aspden, Foster, Kramer and Pavlovic. (see references 14, 15, 21, 24, 30). Additional work at Yawata in Japan by Toguchi and by various workers in other Laboratories have not been listed since this is not intended to be a complete list of the bibliography, but simply one which will give the reader a basic understanding of the problems involved. A great deal of the laboratory work has been on heavy gauge material suitable for large rotating apparatus or for large power transformers. This work continues in the development stage.

PROPERTIES OF THE NEWLY DEVELOPED 0.002" CUBEX ALLOY

The first type of material to become available commercially consists of toroidal cores wound from 0.002" thick CUBEX alloy tape. In Table I the magnetizing force required to establish a given magnetic induction for straight-grain (parallel to the rolling direction) and cross-grain (transverse to the rolling direction) cube-on-edge texture alloys is compared to that required for the CUBEX alloy in which the values are identical for straight-grain and cross-grain (90 degrees from the rolling direction). From the standpoint of permeability at this gauge the CUBEX alloy shows a clear advantage at all inductions, and especially at high inductions, regardless of direction. If one considers an application where the flux path is transverse to the rolling direction the comparison becomes even more striking. For example, at 16 kilogausses the magnetizing force required for the CUBEX alloy is only 1.4 oersteds while that required for the cube-on-edge alloy is 100 oersteds, or over 70 times as much.

Comparison of the residual induction and coercive force from the same tip magnetizing force as shown in Table II may in some respects be unfair to the CUBEX alloy. Since it will have been driven closer to saturation than the cube-on-edge material. For example, at 10 oersteds the CUBEX alloy will have a tip induction of more than 19 kilogausses while in the straight-grain case the cube-on-edge material will reach about 17 kilogausses. Thus, the difference between the residual induction for the straight-grain cube-on-edge material at 15,800 gausses and the residual induction for the straight or cross-grain CUBEX at 11,800 gausses is even more indication of the low remanence of the CUBEX alloy. The Goss texture material taken

cross-grain will reach only about 13 kilogausses at this magnetizing force so a residual induction of 8.5 kilogausses for it is hardly comparable to the other figures. A similar argument can obviously be applied to the values for the coercive force, but any re-evaluation, for example, observing the coercive force from the same tip induction, can only be more flattering to the CUBEX alloy. The magnetic hysteresis loop for the CUBEX alloy has less than 1/2 the width of the straight-grain cube-on-edge hysteresis loop, and less than 1/4 of the width of the cross-grain loop for the cube-on-edge alloy.

From consideration of these data on the two materials it would appear that the CUBEX alloy is superior whether one makes use of the double orientation and the good properties in the cross-grain flux direction or not. For this reason samples were prepared in the form of toroidal cores for further investigation and comparison with toroidal cores made of the Goss texture alloy. Toroidal cores made from the CUBEX alloy tape present no special construction problems. Following procedures worked out long ago for the Goss texture material, cores are wound using standard production techniques. Their edges are bonded with an epoxy resin which imparts a ridigity to the core that makes core boxes unnecessary. Characteristics of toroidal cores of the two materials are compared in Figure 3, which shows the normal d-c magnetization curves for both types and plainly shows the superiority of the CUBEX cores at all inductions but especially at high inductions. Comparing the situation at a magnetizing force of 10 oersteds one sees that the flux density is still over 19 kilogausses in the CUBEX core, but less than 17 kilogausses in the cube-on-edge core.

In the discussion above it was pointed out that the hysteresis loop for the CUBEX alloy was smaller than that for the cube-on-edge alloy by virtue of its lower residual induction and much smaller coercive force. Thus under cyclic excitation one would expect considerably lower hysteresis losses. On the other hand the eddy current losses, which depend principally on the electrical resistivity of the material, should be about equal for the same excitation since both alloys have about the same silicon content and are reasonably pure iron otherwise. If one is concerned only with the classical eddy current losses, which can be equated for these two materials, and the hysteresis losses, which should be lower for the CUBEX alloy, then the CUBEX alloy should have a distinct advantage again. However, there are also differences in the typical arrangements of the magnetic domains in the two materials which might give rise to unanticipated differences in the so called anomalous losses, which are known to be more significant in thinner sheets. Rather than to speculate on this question it is expedient to test cores and determine their total loss characteristics.

The total core loss for the thin CUBEX cores at 400 cycles per second is lower at all inductions than that of the Goss texture cores as shown in Figure 4. As one would expect from the argument presented above, the differences are evident, but not as startling as the differences in d-c properties, because of the strong equal contribution of eddy current losses in both cases. Even so, especially at the higher inductions, the CUBEX cores are remarkably lower in loss than the Goss textured cores. At 15 kilogausses the 400 cycle core loss in watts per pound is 8.0 for Goss texture cores and is

only 5.5 for CUBEX cores, an improvement of 31 percent.

The exciting RMS volt-amperes required for CUBEX cores, although equivalent to cube-on-edge cores at low inductions, are again lower at high inductions. From Figure 5 one can see that at 15 kilogausses the 400 cycle exciting rms volt amperes per pound is 6.5 for the CUBEX cores and about 12 for Goss texture cores.

At higher frequencies CUBEX cores retain their advantage over cube-on-edge cores. For example, at 2,000 cycles per second and 15 kilogausses the watts lost per pound of material are 48 for CUBEX cores and 59 for cube-on-edge cores, an 18 percent advantage for the CUBEX cores. Under the same conditions the exciting RMS volt amperes per pound are 50 for CUBEX cores and 68 for Goss texture cores. The evident superiority of the CUBEX cores make them clearly desirable for any applications such as those in the aerospace field, where performance is crucial. It is also fairly clear that by proper core selection and core winding design considerable savings in space, weight, and efficiency may be obtained.

Magnetic Field Annealing

The magnetic properties of CUBEX toroidal cores respond favorably to an annealing treatment in a magnetic field. If cores are annealed without a magnetic field there is no substantial degree of common alignment of magnetic domains, but with the magnetic field, the alignment of domains can be established in either the rolling direction

or 90 degrees to it, according to what the application may require. Cores were cooled from an elevated temperature in an Inconel retort at a predetermined rate in a dry hydrogen atmosphere in the presence of a field of 10 oersteds provided in the direction of the toroidal windings (along the rolling direction) by a single turn fixture which is attached to the seal at the cold end of the Inconel retort.

The domain alignment in cores which are annealed in a magnetic field generates a marked improvement in magnetic properties. The magnetization curves of a CUBEX core before and after a field anneal are shown in Figure 6. There is a noticeable increase in rectangularity of the magnetization curve after magnetic annealing. The maximum permeability increased from 22,590 to 73,170 and, as one might expect, a corresponding increase in the residual induction (measured from a tip magnetizing force of 10 oersteds) from 11,800 to 17,960 was found after the magnetic anneal. Losses and exciting volt amperes were also improved by this treatment. For example, the 400 cycle losses at 15 kilogausses dropped from 5.5 watts per pound with a normal stress-relief anneal to 4.5 watts per pound after the magnetic anneal, an improvement of about 18 percent. Unfortunately Goss texture cores annealed in a magnetic field do not change appreciably.

Properties of the CUBEX alloy cores in the stress-relief annealed and magnetically annealed conditions are compared with several specialty alloys in the nickel-iron and cobalt-iron families in Figure 7. From the standpoint of application of material it is evident from the preceding paragraphs that the CUBEX alloy cores can be considered for many applications now using the Goss texture silicon iron alloys, and

from an examination of Figure 7, there appear to be areas where the CUBEX cores may replace either the isotropic 49 percent nickel-iron or the sharp kneed (almost rectangular hysteresis loop) 50-50 nickel-iron. If a design calls for operating induction of 15.5 kilogausses and a magnetizing force of 1 oersted, non-field annealed CUBEX cores may be a substitute for either the oriented or unoriented nickel iron. Magnetically annealed CUBEX cores could serve where oriented 50-50 nickel-iron could not, if the design requirements were more restrictive, say 16 kilogausses at 0.3 oersted, since the curve for the field annealed CUBEX cores is 1 kilogauss above the curve for the oriented 50-50 nickel-iron curve at that magnetizing force. Except for extremes of induction or extremes of temperature either type of CUBEX core could replace the 27 percent cobalt-iron cores and below about 17.5 kilogausses the field annealed CUBEX alloy cores are superior to Supermendur (50-50 cobalt-iron) cores as well.

CONCLUSIONS

The properties of the CUBEX alloy cores appear sufficiently competitive to the properties of the other specialty alloys that they may be expected to replace several of the special materials, depending upon design factors, in such apparatus as saturable reactors, or magnetic amplifiers, servo devices, torque motors, microsyn generators, instrument transformers, intermediate frequency transformers and other devices generally using specialty magnetic materials.

The applications to magnetic amplifiers, inverters, and to pulse cores are being studied at the present time. On the basis of preliminary data it appears that the CUBEX alloy cores possess a high pulse permeability and will, therefore, be useful in pulse core

applications. After field annealing the CUBEX alloy appears to be useful for magnetic amplifiers. For example, at a magnetizing force of 1 oersted it is possible to operate CUBEX at higher inductions while maintaining the control current below the level normally used with nickel-iron cores.

To summarize the situation briefly the CUBEX alloy cores are shown to have a higher permeability and better d-c characteristics than Goss texture silicon-iron cores and under a-c conditions are shown to have lower losses and require less exciting current at 400 cycles and 2000 cycles. Thus in many applications the CUBEX cores may be considered for replacing the Goss texture cores with some technical advantages. It also appears possible to make similar substitutions with some of the specialty magnetic materials of the nickel-iron and cobalt-iron types. Thus on the basis of initial tests a number of applications should benefit from the use of CUBEX cores possibly including pulse cores and magnetic amplifiers.

ACKNOWLEDGEMENTS

The author wishes to express his appreciation to Mr. Norman Pavlik who did much of the preparatory work for this paper, to the Armco Steel Corporation, for furnishing the CUBEX alloy tape used in these investigations, and to the people at the laboratory who assisted Mr. Pavlik in his endeavors, especially J. F. Fritz, J. J. Clark, G. W. Wiener, R. D. Olson and R. G. Aspden.

REFERENCES

1. The Magnetic Properties of Fe Crystals at Ordinary Temperature, K. Beck, Zurich Naturforsch. Ges. 63, 116-186, 1918

2. Magnetic Properties of Single Crystals of Si-Fe, H. J. Williams, Phys. Rev. 52, 747-51, 1937.

3. Magnetic Anisotropy of Single Crystals of Fe and Ni, H. Schlechtweg, Ann. Physik, (5) 27, 573-96, 1936

4. Calculations of Torque on a Ferromagnetic Single Crystal in a Magnetic Field, R. M. Bozorth, H. J. Williams, Phys. Rev. 59 827-33, 1941.

5. U. S. Patent 1,965,559 1934 (Appli. 8-7-33) Electrical Sheet and Method and Apparatus for its Manufacture and Test. New Development in Electrolytic Strip Steels Characterized by Fine Grain Structure Approaching Properties of a Single Crystal, Trans. Am. Soc. Metals 23, 515-31, 1935. U. S. Patents 2,084,336 and 2,084,337 (Appl. 1-30-34, 12-1-34) Magnetic Material and Method of Manufacture (1937). N. P. Goss

6. Orientation of Crystals in Silicon-Iron, R. M. Bozorth. Am. Soc. Metals, 23, 1107-1111, 1935

7. Magnetic Material and Method of Producing Same, A. A. Frey, F. Bitter. U. S. Patent 2,112,084 (Appl. 11-1-34)

8. Art of Producing Magnetic Materials, G. H. Cole, R. L. Davidson. U. S. Patent 2,158,065, (Appl. 1-9-35).

9. Method of Producing Silicon Steel Sheet or Strip, U. S. Patent 2,236, 519 (Appl. 1-22-36); Process of Producing High Permeability Silicon Steel, U. S. Patent 2,287,466 (Appl. 12-5-39), V. W. Carpenter.

10. Magnetic Anisotropy in Silicon Steel, K. J. Sixtus. Physica 6, 105-111, 1935.

11. Magnetic Properties of Fe-Al Alloys, R. M. Bozorth, H. J. Williams, R. J. Morris. Phys. Rev. 58 203, 1940.

12. On Iron-Silicon with Cube Texture, I-Magnetic Investigation, F. Assmus, R. Boll, D. Ganz, and F. Pfeifer. Zeitschrift für Metallkunde, 48, 341-343, 1957.

13. On Iron-Silicon with Cube Texture, II - Development of the Texture, F. Assmus, K. Detert, and G. Ibe. Zeitschrift für Metallkunde, 48, 344-349, 1957.

14. Cube Texture in Body Centered Magnetic Alloys, G. W. Wiener, P. A. Albert, R. H. Trapp, and M. F. Littmann. Jnl. Appl. Phys., 29, 366-7, 1958

15. Cube Oriented Magnetic Sheet; a Major Advance in Magnetic Materials, G. W. Wiener, K. Detert. Jnl. of Metals, 10, 507-8, Aug., 1958.

16. Magnetic Properties of Cube Textured Silicon-Iron Magnetic Sheet, J. L. Walter, W. R. Hibbard, H. C. Fiedler, H. E. Grenoble, R. H. Pry, P.G. Frischmann, Jnl. of Appl. Phys., 29, 363-5, 1958, Jnl. of Metals 10, 509-11, Aug., 1958.

17. Texture of Cold-Rolled and Recrystallized Crystals of Silicon-Iron, J. L. Walter, W. R. Hibbard, Jr. Trans AIME 212, (6), 731-7, Dec., 1958.

18. Secondary Recrystallization in Silicon-Iron, J. E. May, D. Turnbull Trans. AIME 212, (6), 769-81, Dec., 1958.

19. Development of Metallurgical Structures and Magnetic Properties in Iron-Silicon Alloys, R. H. Pry. Jnl. Appl. Phys. 30, 189S- 193S April, 1959.

20. Tertiary Recrystallization in Silicon Iron, J. L. Walter, C. G. Dunn. Trans. Am. Inst. Met. Eng. 215, 465-71, 1959.

21. Influence of Constraints During Rolling on Texture of 3 Percent Silicon-Iron Crystals Initially (001) [100] , R. G. Aspden. Trans. AIME, 215 (6), 986-91, 1959.

22. Investigation of a New Kind of Secondary Recrystallization in 3 Percent Silicon-Iron Alloys, K. Detert. Acta Met. 7, 589-98, 1959.

23. Bloch Wall Spacing in Thin Si-Fe Samples with Cube Texture, R. Brenner. Zeitschrift für Angewandte Physik, 12, 107-11, 1960

24. Effect of Directional Orientation on the Magnetic Properties of Cube-Oriented Magnetic Sheets, K. Foster, J. J. Kramer. Jnl. Appl. Phys. 31, 233S-4S, 1950.

25. Secondary Recrystallization in Vacuum Annealed Silicon-Iron, G. Baer, D. Ganz, H. Thomas. Jnl. Appl. Phys. 31, 235S-6S, 1960.

26. Promotion of Cubic Grain Growth in 3 Percent Silicon Iron by Control of Annealing Atmosphere Composition, D. Kohler. Jnl. Appl. Phys. 31, (5), 408S-409S, 1960.

27. Effect of Impurity Atoms on Energy Relationship of (100) and (110) Surfaces in High-Purity Silicon-Iron, J. L. Walter, C. G. Dunn. Acta Metallurgica, 8, 497-503, 1960.

28. Nature of Matrix for Secondary Recrystallization to Cube Texture in High-Purity Silicon-Iron, C. G. Dunn, J. L. Walter. Trans. AIME, 218, 448-53, 1960.

29. Growth Behavior of Cube-Oriented Secondary Recrystallization Nuclei in High-Purity Silicon-Iron, J. L. Walter, C. G. Dunn. Trans. AIME 218, (5), 914-22, 1960.

30. Magnetic Properties of Oriented 3 Percent Aluminum Iron Sheets, K, Foster, D. Pavlovic. Jnl. Appl. Phys., 34, 1325-6, 1963.

TABLE I

MAGNETIZING FORCES REQUIRED TO ESTABLISH A GIVEN MAGNETIC INDUCTION IN 0.002 INCH THICK SILICON-IRON ALLOYS

CUBE-ON-EDGE ALLOY COMPARED TO CUBE TEXTURE ALLOY

INDUCTION IN KILOGAUSSES, B	MAGNETIZING FORCE, H, IN OERSTEDS		
	CUBE-ON-EDGE ALLOY (GOSS TEXTURE)		CUBE TEXTURE ALLOY (CUBEX ALLOY)
	ROLLING DIRECTION	TRANSVERSE DIRECTION	ROLLING DIRECTION AND TRANSVERSE DIRECTION
3	0.39	1.49	0.21
6	0.48	2.0	.29
9	0.57	2.45	.41
12	0.68	4.70	.54
15	1.2	64.0	.84
16	2.6	100	1.4
18	30	------	2.3
19	60	------	6.4

TABLE II

A-C PROPERTIES OF 0.002 INCH THICK SILICON-IRON ALLOYS
CUBE-ON-EDGE ALLOY COMPARED TO CUBE TEXTURE ALLOY

MAGNETIC PROPERTY	CUBE-ON-EDGE ALLOY (GOSS TEXTURE)		CUBE TEXTURE ALLOY (CUBEX ALLOY)
	ROLLING DIRECTION	TRANSVERSE DIRECTION	ROLLING DIRECTION AND TRANSVERSE DIRECTION
MAXIMUM PERMEABILITY	20,000	3,800	22,600
RESIDUAL INDUCTION,* GUASSES	15,800	8,500	11,800
COERCIVE FORCE,* OERSTEDS	0.55	0.97	0.24

*(AFTER A TIP MAGNETIZING FORCE OF 10 OERSTEDS)

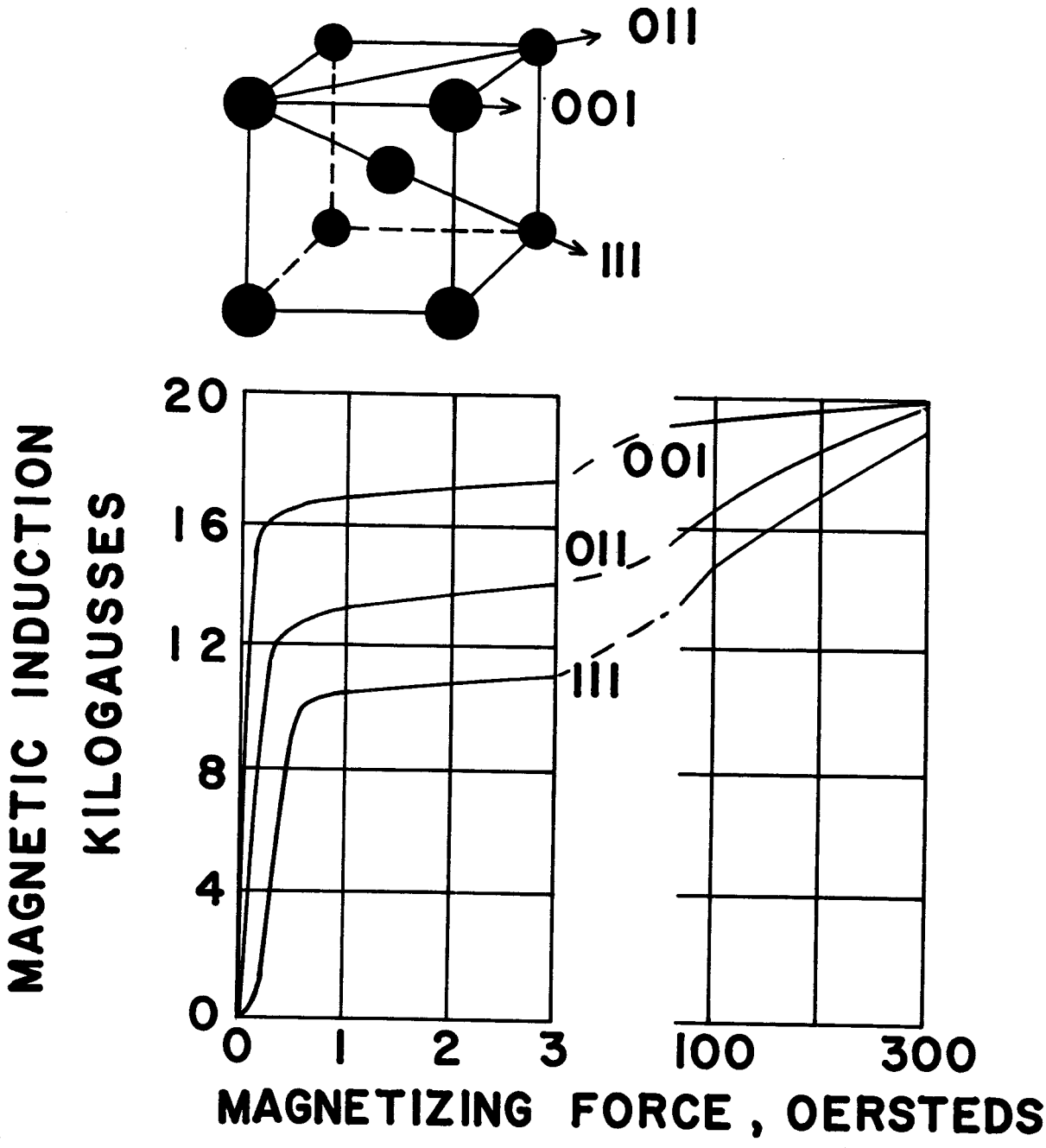

Figure I. Relation Between the Principal Crystallographic Directions and the Corresponding Magnetic Properties of Iron Single Crystal

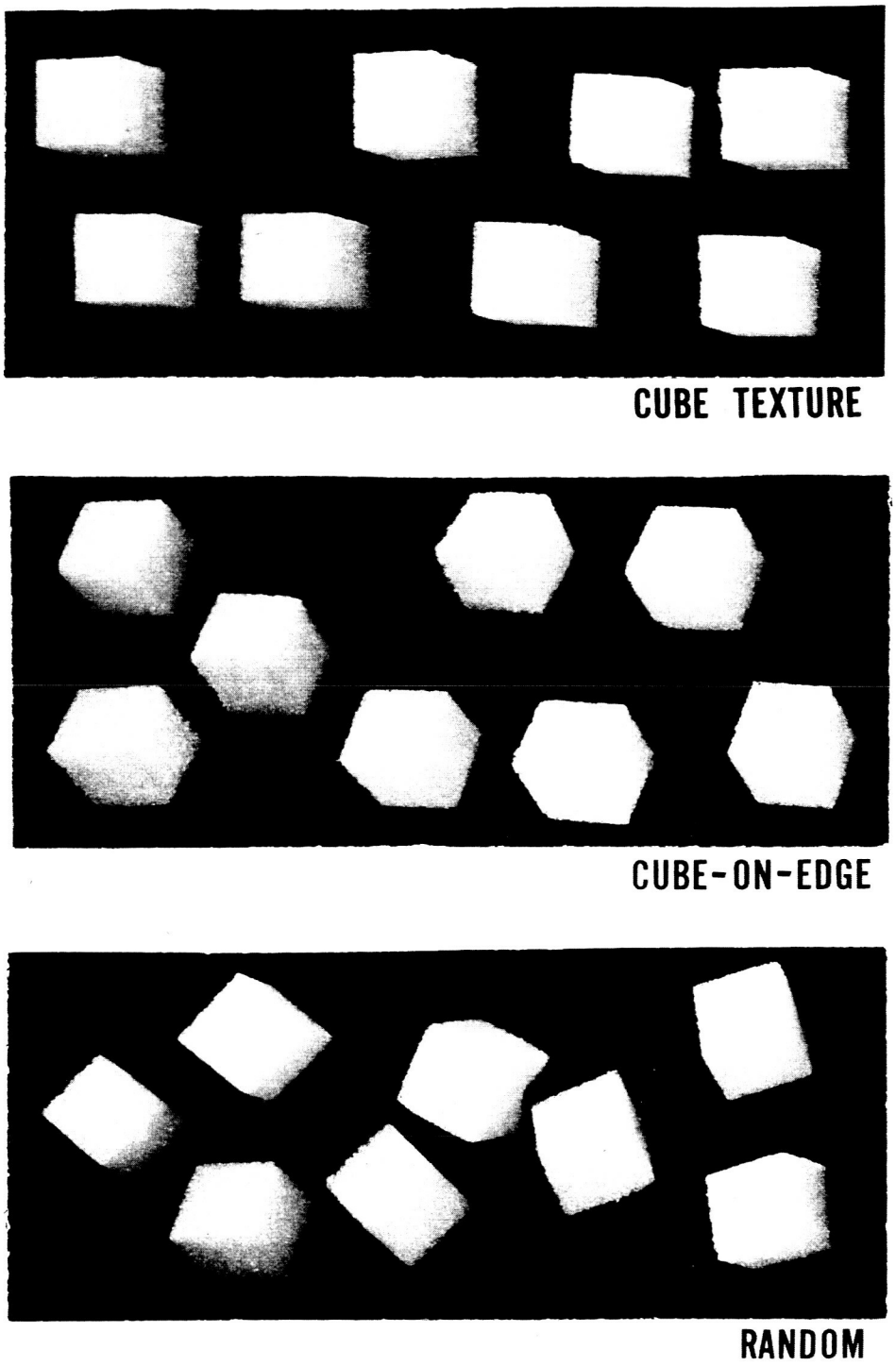

Figure 2. Models Showing the Alignment of Iron Cubic Crystals with Respect to the Rolling Direction of a Sheet of Steel for Three Types of Orientation: Common or Random, Cube-on-Edge, and Cube Texture

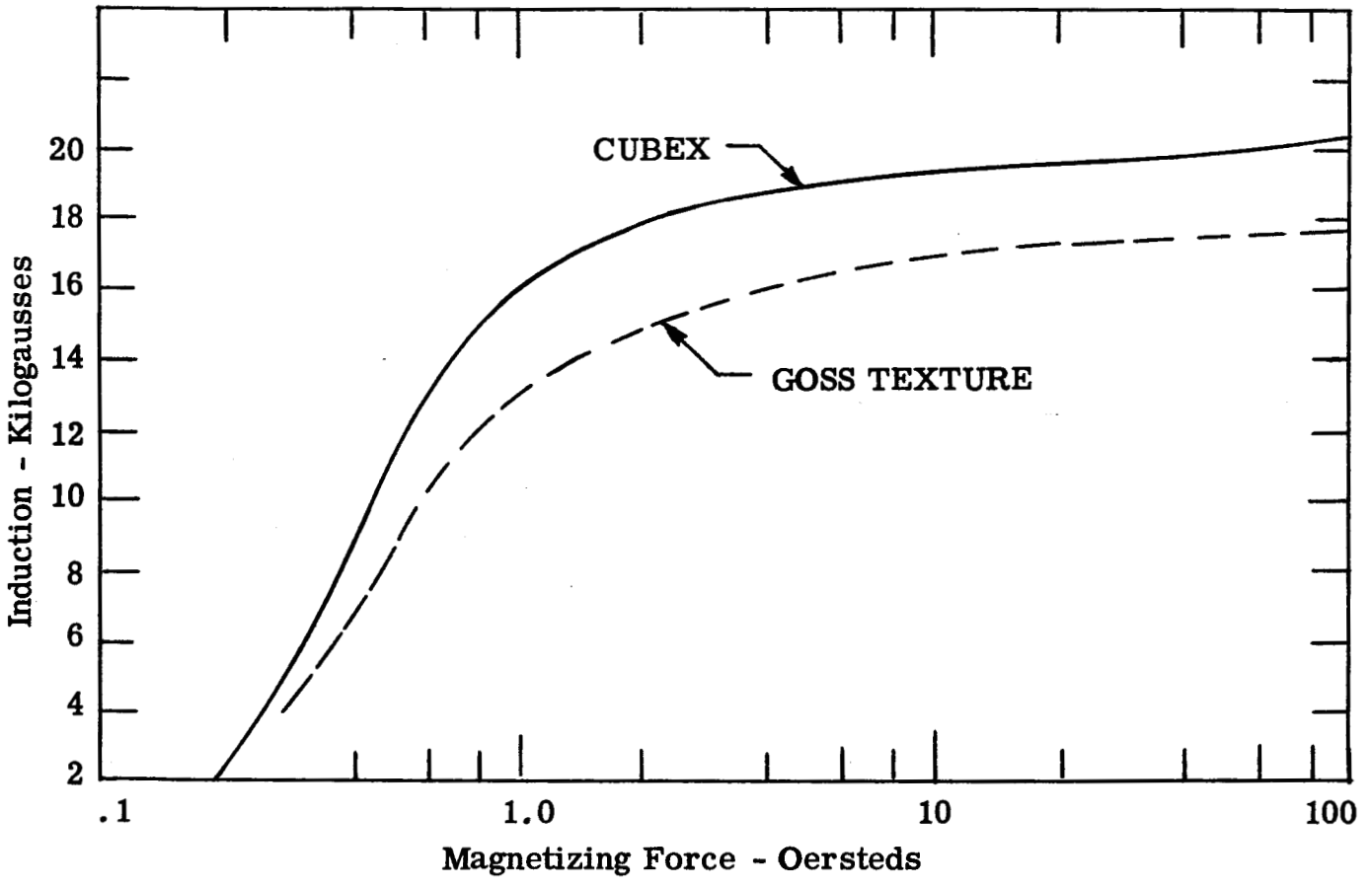

Figure 3. Normal Magnetization Curves for Cube Texture and Goss Texture .002 Inch Tape Wound Cores

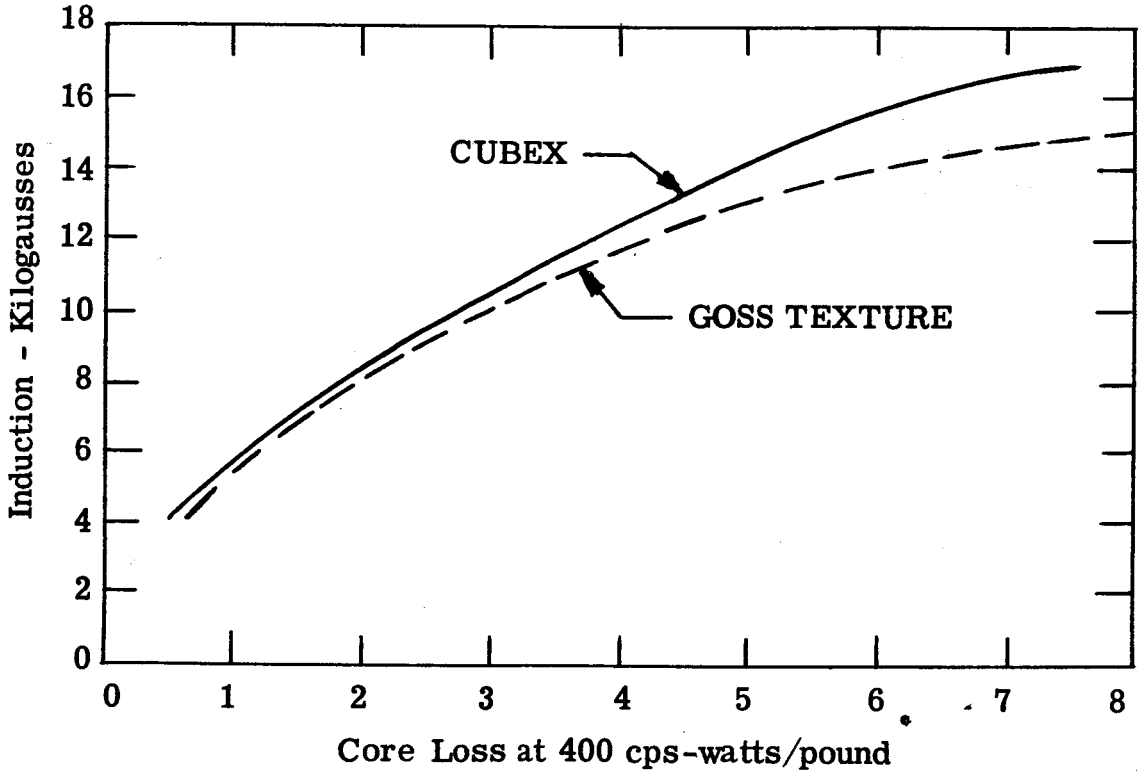

Figure 4. 400 Cycle AC Core Lose Curves Comparing Cube Texture and Goss Texture .002 Inch Tape Wound Cores

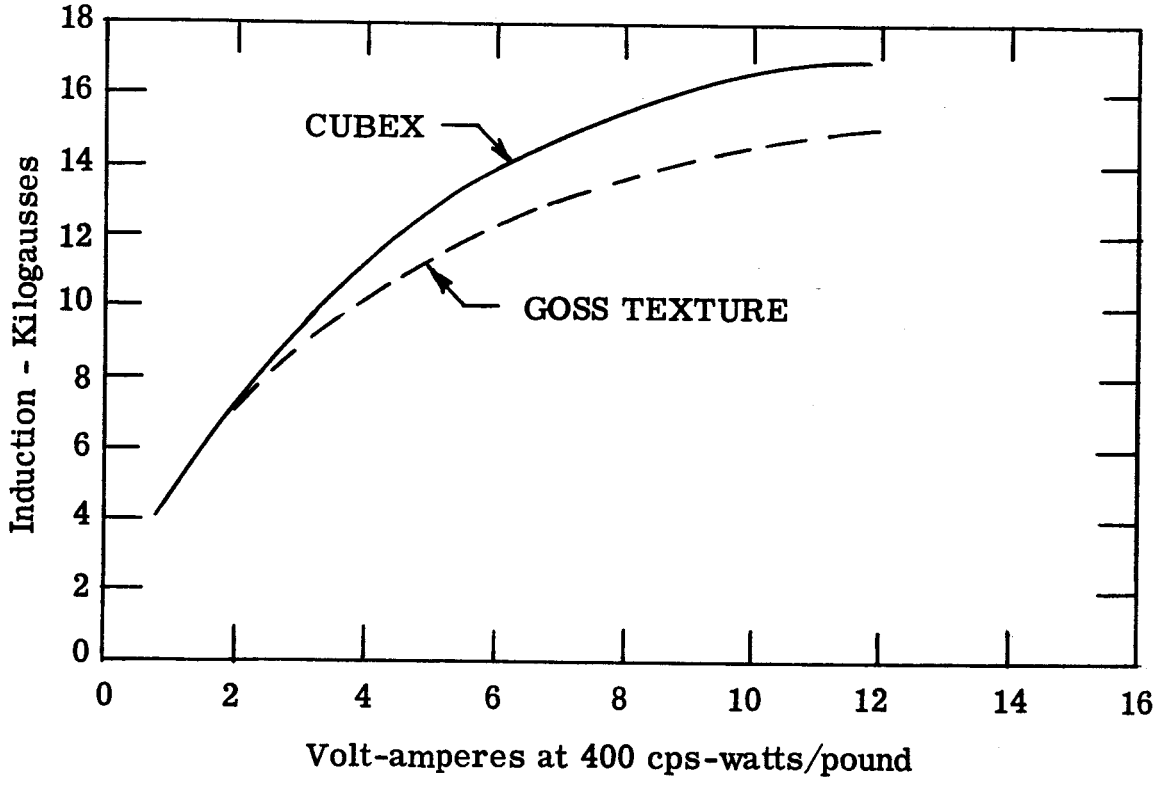

Figure 5. 400 Cycle AC Exciting Volt Ampere Curves Comparing Cube Texture and Goss Texture .002 Inch Tape Wound Cores

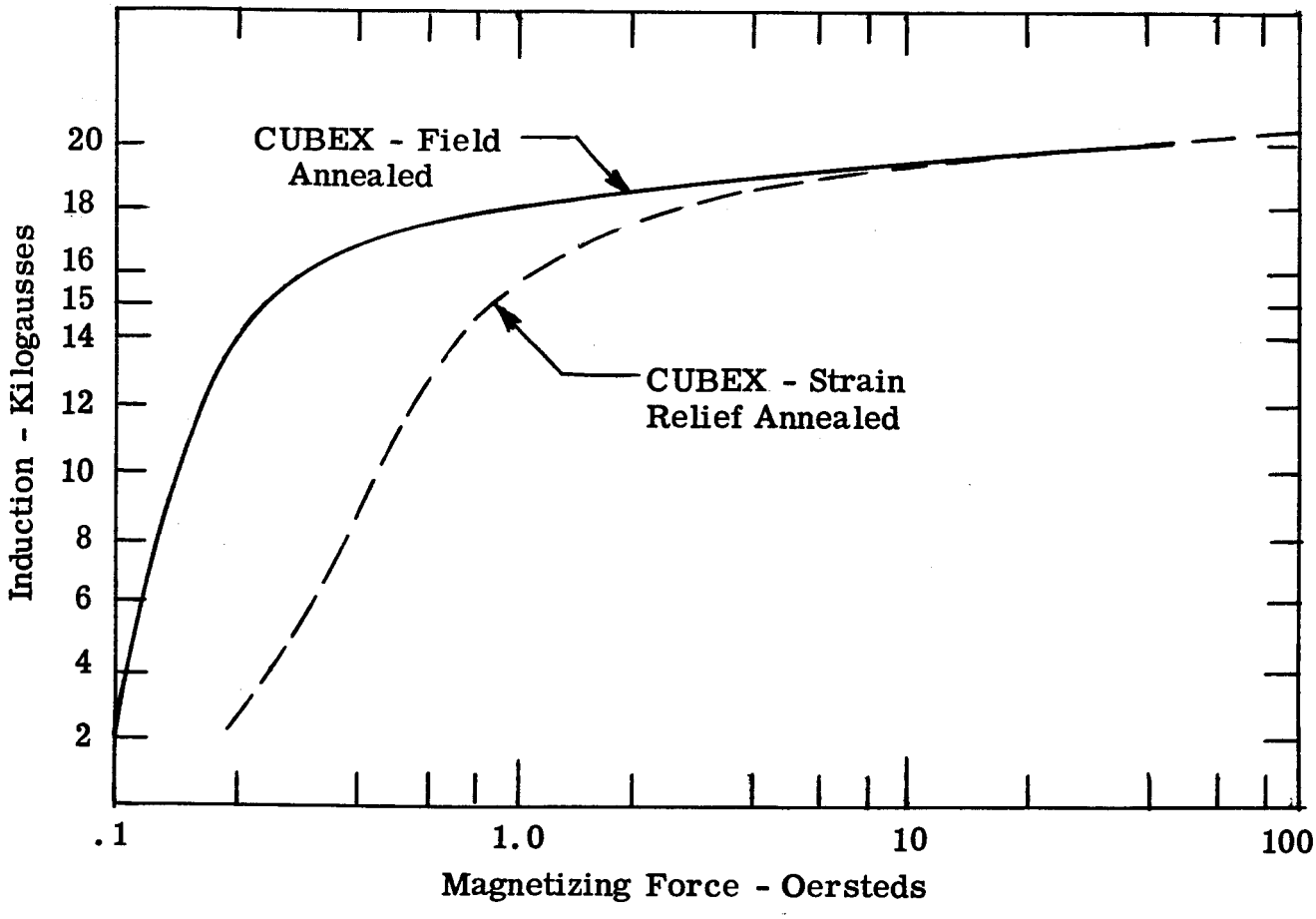

Figure 6. Normal Magnetization Curves Comparing Cube Texture Field Annealed .002 Inch Tape Wound Cores with Strain Relief Annealed Cores

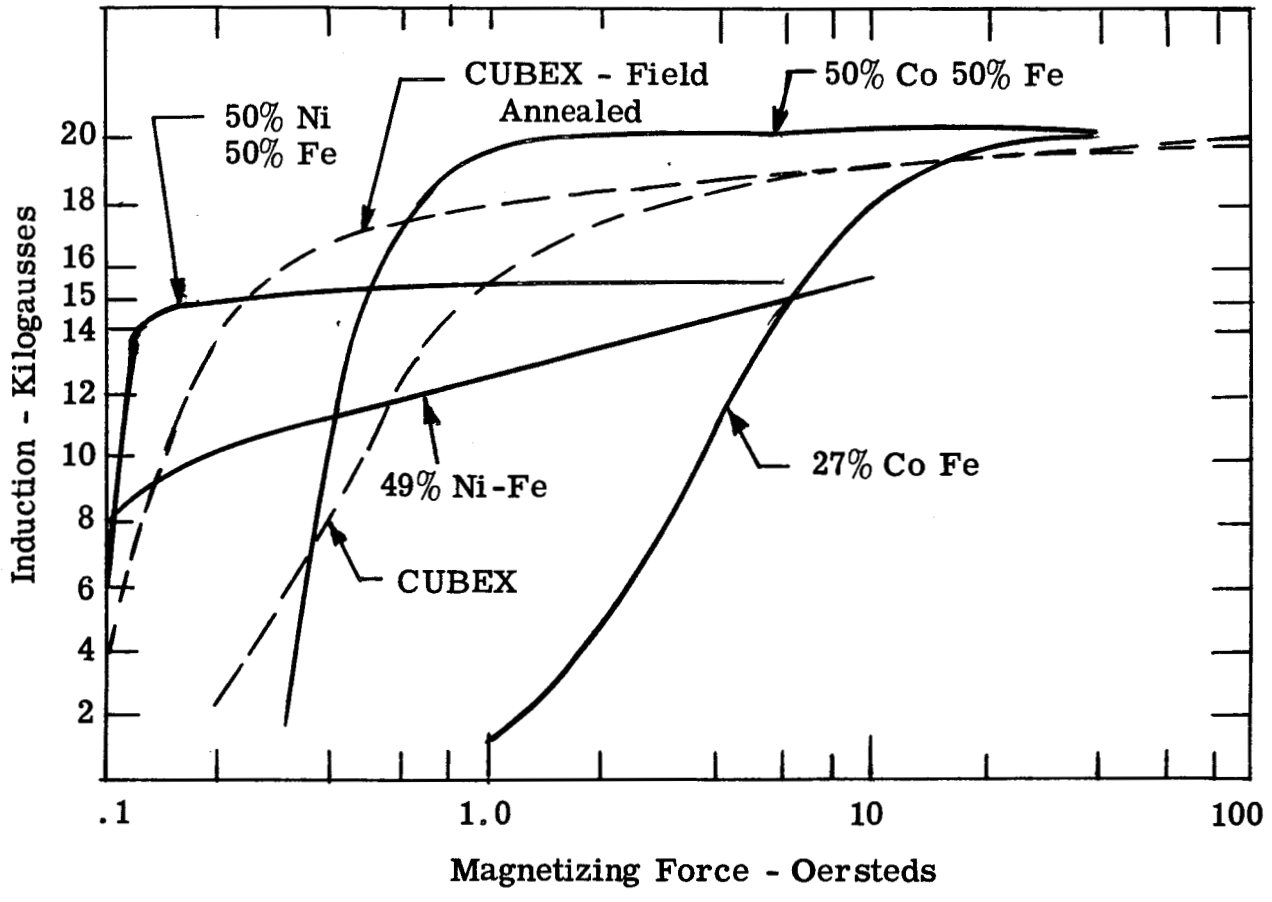

Figure 7. Normal Magnetization Curves Comparing CUBEX Field Annealed and Strain Relief Annealed Cores with Some Common Specialty Alloys

APPENDIX II

LABORATORY TEST SPECIFICATION FOR TRANSFORMER AND PARALLELING EVALUATION

SM 11-61 LPLCO

SPECIFICATIONS FOR LABORATORY TEST No. N4-202

☐ Dept. 81. (Engr. to send all four copies to lab.) Lab. adds cost and schedule and returns 2 copies to:

☐ _____ Engr. Dept.—Eng. Dept. clerk distributes:

☐ 1 copy to Section File ☐ 1 copy to Engr. Mgr.

FILE—Del. Fol. Section after above is crossed out.

20006-1B
Scheduled SE/PE 20006-2B Priority _____

Trouble Docket or Development Project No. _____

Sample LY P18292 & 3 Charge See Below

Test LY _____ Eng. Test _____

Hours _____ $ _____ Start _____ Cpt. _____

Frame/Type _____ Rotation _____ (End opposite shaft)

P/N _____ G. O. CLD 22790

Customer _____

Style _____ Section _____

APPARATUS: (2) Inverter/Converter Models (P/N LYP18293J1 and (1) Transformer (P/N LYP18292D1)

OBJECT: (1) To demonstrate feasibility of paralleling inverters & converters. (2) To evaluate performance of a transformer utilizing field annealed doubly oriented silicon-iron in an inverter circuit and compare results with those of conventional transformer core materials.

OUTLINE _____ Line Wiring Diag. _____ Diag. WAF _____ AC DC _____ Wd.

RATING _____ KW HP KVA _____ V _____ A _____ rated rpm. _____ max. rpm. _____ Ph. _____ Cy.

Res. _____ °C: Arm _____ Main Shunt _____ Aux. Series _____ Comp. _____ I.P. _____ Total Coil _____ Check and record all rea.

Excitation _____ V _____ A. Brush Setting _____ (After running in brushes.)

Winding Off Neutral _____ bars CW. _____ CCW. _____ bars. Comm. Brake tests at fld. temp. _____ °C. Ground test 60 cy., 1 sec. _____ V.

Brushes: No. _____ Grade _____ Size _____ lg. _____ w. _____ tk. Dwg. _____ Ounces pressure _____

Ventilation: Self Forced Open Encl. _____ CFM. _____ inches water Dia. tube _____ Special Enclosure _____

Capacitor: _____ mfds. S No. _____ Thermoguard Spencer No. _____ Switch Op. Speed _____

Comm. test is/is not to be approved prior to curve test. Govt. witness test: USAF _____ USN _____ None _____

Test Specs. _____ Other test letters, on same unit or set-up _____

Record Data on Forms _____ Plot Curves _____ Check Weight _____

DISPOSITION AFTER TEST: Engineering Storeroom

INSTRUCTIONS and PROCEDURE: (Engineer to requisition all associated apparatus listed below. Laboratory to provide all test equipment required to perform tests.)

Sections 1, 2, 3, 4, and 5: (Charge E2N-5()-LYP18293)

Section 6: (Charge E2N-5()-LYP18292)

Signed G.W.Ernsberger G W Ernsberger Engineer—Date 1.10.64 Test No. N4-202

Approved R.L.Gasperetti Section Manager _____ Sub. _____

Test Equipment Required

No.	Description
2	0-32 volt, 35 amp, d-c power supply (E1, E2)
2	0-30 volt, d-c voltmeter
2	0-50 amp d-c ammeter
1	Oscilloscope, 10 Mc, dual channel
1	3 phase circuit breaker, 10 amps, 150 volts
2	DC vacuum tube voltmeters 0-30 volt
2	3 phase, 400 cps, 115V, 0-500VA/Ø, P.F. 0.9 leading to 0.5 lagging, load bank
2	0-150V a-c rms voltmeter
6	0-5 amp a-c ammeter
6	0-500 watt a-c wattmeter
2	Frequency counter
2	Selector switch box for voltmeters
1	Recording oscillograph
2	0-200V d-c voltmeter
2	0-10 amp, d-c ammeter
2	0-1000 watt d-c wattmeter

Unless otherwise specified instrument accuracy shall be as follows:

(a)	Frequency	±1 cycle
(b)	RMS voltage	±.25%
(c)	DC voltage	±.25%
(d)	RMS current	±.25%
(e)	DC Current	±.25%
(f)	Watts	±.25%

1.0 Measurement of Reactive Load Division Circuit Loop Gain.

Connect inverter model in test circuit described in Figure 8. Set input d-c voltage (E1) at 28 ± 1 volts.

1.1 Connect a three phase load on output terminals A2, B2, and C2 to N (Figure 8) such that the output load current is 1.0 PU, (2.18 amps/phase) .5 PF lagging. Measure the output voltages. These voltages should be 67.5 ± 10 volts rms line-to-neutral. Record the output voltages, currents and watts under this condition.

NOTE: The output voltage should decrease as the load current is increased. Therefore, the impedance of the load will have to be reduced accordingly to obtain 1.0 PU output current under these conditions.

2.0 Test of Frequency Lock Circuits.

2.1 Connect two inverters as shown in Figure 9. Do not connect d-c power supplies as shown in Figure 9. Open all switches. It is not necessary to connect the load nor output meters for this test of frequency lock circuits.

2.2 Disconnect d-c power from the power stages of the inverters.

2.3 Connect the + lead of a variable voltage d-c power supply through a switch to the input terminal (+INP). Use a separate d-c power supply for each inverter. Connect the negative lead of the d-c power supplies to (-INP) terminals.

2.4 Close switches K1, K2, and K3.

2.5 Connect a d-c vacuum tube voltmeter across the collector of transistor Q24 to (-INP) on each inverter. (These meters are indicators only and need not exceed ± 10% accuracy.)

2.6 Set the voltage on each d-c power supply at 28 ± 2 volts and apply d-c voltage to both inverters simultaneously.

2.7 One of the collectors of Q24 to (-INP) voltages should rise to 19 ± 1 volts while the other should rise to 3 ± 1 volts.

2.8 Connect a separate d-c power supply from base to emitter on Q25 on the inverter whose Q24 collector to (-INP) voltage is 3 ± 1 volts. Raise the base to emitter voltage on the Q25 until the voltage from the collector of Q24 to (-INP) on that inverter changes from 3 ± 1 volts to 19 ± 1 volts. The same voltage on the other inverter should reduce from 19 ± 1 volts to 3 ± 1 volts. There should be no further change when the separate power supply is disconnected from base to emitter of Q25.

2.9 Disconnect the voltmeters from the collector of Q24 and connect a dual channel oscilloscope to the collector of Q4 on both inverters. Set the oscilloscope on chopped, dual channel operation. Connect the common side of the oscilloscope to the (-INP) terminal. The collector of Q4 voltage on each inverter should be operating at the same frequency and in phase. Photograph the oscilloscope output to record this frequency locked condition.

3.0 Test of Phase Lock Circuits.

3.1 After completing Section 2.0, disconnect the oscilloscope from the collector of Q24 on each inverter. Connect the oscilloscope to the collector of transistor Q17A to (-INP) on each inverter. The voltage across each Q17A should be a square wave of the same frequency but not necessarily in phase with each other. Photograph the oscillograph picture to record the out-of-phase condition.

3.2 Close switch K4. This connects together the "H" terminals of both inverters and should lock both countdown circuits in phase with each other. The square wave voltages seen on the oscilloscope must now be in phase with each other. Photograph the oscilloscope picture to record the in-phase condition.

3.3 Disconnect the d-c power supplies.

4.0 Parallel Inverter Operation

4.1 Reconnect the inverter power stages to the d-c input which were disconnected in Section 2.2. Finish connecting the two inverters in parallel as shown in Figure 9.

4.1.1 Connect voltmeters, ammeters, wattmeters, and a frequency meter on each inverter output. Rated load current is 2.18 amperes.

4.1.2 Connect a separate 0-350 VA per phase, 0.9 leading to 0.75 lagging load to each inverter through a 3 PST switch.

4.1.3 Parallel the loads through an aircraft circuit breaker. Connect auxiliary contacts to short X1 to X2 on both inverters when the main contacts are open. This will disable the load division circuit during isolated operation.

4.1.4 Connect an ammeter and a voltmeter on each inverter input. Maximum d-c current is 50 amperes. Voltage varies from 26.0 to 30.0 volts d-c.

4.1.5 Open all switches and the paralleling circuit breaker.

4.2 Close switches K1, K2, and K3 to lock the frequency reference together.

4.3 Set loads at no load on each inverter. Close load switches to individual inverters but do not parallel the loads.

4.4 Connect one channel of a two channel oscilloscope to the collector of Q4 and (-INP) on inverter I. Connect the other channel to the collector of Q4 and (-INP) on inverter II.

4.5 Set both input d-c power supply voltages at 28 ± 2 volts and apply these voltages to the inverter.

4.6 When both Q4's operate at the same frequency, close switch K4 to lock the inverters in phase with each other.

4.7 Measure the voltage between V_{AI} and V_{AII}, V_{BI} and V_{BII}, V_{CI} and V_{CII}. These voltages must be 0 ± 2 volts. If they are not, adjust the appropriate R15. All line to neutral voltages on each inverter must be 115 ± 1 volt.

4.8 If the requirements of 4.7 are met, parallel the loads by closing the paralleling circuit breaker.

4.9 Operate the inverters in parallel and record the following data:

Load terminal voltages, 3Ø, L-N
Individual output currents
Individual output watts
Output frequency
Input voltage
Input current

4.9.1 Use the following loads:
0%
25%
50%
75%
100%
125%
at each of the following power factors:
.9 leading
1.0
.9 lagging
.75

NOTE: 100% load equals 250 VA per phase per inverter.

4.10 Repeat 4.3 through 4.8 except set the loads at those required in 4.9.1.

4.11 Using a recording oscillograph, record both phase A inverter output currents and voltages during the four 100% load paralleling transients required in section 4.10.

4.12 To demonstrate that an unloaded inverter can be paralleled with a loaded inverter, repeat 4.3 through 4.11 with one inverter unloaded and with the other inverter loaded to 100%, 1.0 PF. Record data called for in section 4.9 before and after paralleling. Use a recording oscillograph to record both phase A inverter output current and voltages during the paralleling transient.

4.13 To demonstrate that large load transients can be sustained by the paralleled inverters, parallel the unloaded inverters; then, simultaneously, apply two 100% 1.0 PF loads to the paralleled inverters. Record the data indicated in section 4.9 before and after applying the load. Use a recording oscillograph to record both phase A inverter output current and voltages during the application and removal of the load.

5.0 Single Converter Operation Test

5.1 Make terminal connections as shown in Figure 10. This connects the inverter output in delta and rectifies it through a three-phase full-wave rectifier. The output of the rectifier is connected to the + and - output terminals. Connect d-c output voltage, current, and wattmeters to these output terminals.

5.2 Connect a resistive load of 31.5 ohms (750 watt) across the output terminals.

5.3 Connect the d-c input source (E1) through a contactor to the input terminals. Set E1 at 28.0 ± 1.0 volts with the contactor open.

5.4 Close the input contactor.

5.5 Set the output voltage at 153.5 ± 1 volts d-c by adjusting potentiometer R15. Output current should be 4.88 amperes. Adjust load impedance, if necessary, to obtain this current.

5.6 Adjust the voltage across R69 to $20 \pm .1$ volts by adjusting R69. This adjustment establishes the transfer characteristics of the d-c current transducer in the d-c load division circuit so that one per unit load current (4.88 amps) is proportional to 20 volts between terminals Y1 and Y2.

5.7 Record the voltage across R69 for load currents from 0 to 6 amps by changing the load current in one ampere steps.

5.8 Repeat sections 5.0 through 5.7 for the second converter.

6.0 Parallel Converter Operation Test.

6.1 Connect two converters as shown in Figure 11.

6.1.1 Connect d-c voltmeters, ammeters, and wattmeters to each converter output. Rated current is 4.88 amperes d-c.

6.1.2 Connect a separate 0 to 1000 watt load to each converter through SPST switch.

6.1.3 Parallel the loads through an aircraft circuit breaker. Switch K6 is an auxiliary contact on this circuit breaker which closes when the main contacts are closed.

6.1.4 Connect a d-c voltmeter and ammeter to each converter input. Maximum d-c current is 50 amperes. Voltage varies between 26.0 and 30 volts d-c.

6.1.5 Open all switches and the paralleling circuit breaker.

6.2 Set both input d-c power supply voltages at 28± 2volts d-c and apply these voltages to the converter input terminals.

6.3 Measure the voltage across the circuit breaker contacts. If this voltage is 0± 2 volt, close the circuit breaker.

6.4 Operate the converters in parallel and record the following data:

Output terminal voltage
Individual output currents
Individual output watts

6.4.1 Connect the following loads to each converter before closing the paralleling circuit breaker.

0%, 25%, 50%, 75%, 100%, 125%

NOTE: 100% load equals 750 watts/converter.

6.5 Using a recording oscillograph, record both converter output voltages and currents during the six paralleling transients of section 6.4.

6.6 To demonstrate that an unloaded converter can be paralleled with a loaded converter, parallel an unloaded converter with a converter loaded to 750 watts. Record data in accordance with section

6.4 before and after paralleling. Use a recording oscillograph to record both converter output currents and voltages during the paralleling transient.

6.7 To demonstrate that large load transients can be sustained by the paralleled converters, parallel the unloaded converters; then, simultaneously, apply two 750 watt loads to the paralleled converters. Record data in accordance with section 6.4 before and after applying the load. Use a recording oscillograph to record both converter output currents and voltage during the application and removal of the load.

7.0 Comparison Between Conventional Core Materials and "Cubex" Core Material in Output Transformer.

7.1 Connect one inverter as shown in Figure 8.

7.1.1 Connect input d-c voltmeter, ammeter, and wattmeter. Input voltage 26.0 to 30.0 volts. Maximum input current is 50 amperes.

7.1.2 Connect a complete set of three phase voltmeter, ammeters, and wattmeters. Rated output voltage is 115 volts rms line-to-neutral. Rated current is 2.18 amperes per phase.

7.1.3 Connect a 0 to 350 VA per phase, .9 leading to .75 lagging load to the output terminals.

7.1.4 Set d-c input voltage (E1) to 28 ± .1 volts d-c.

7.2 Perform sections 4.9 and 4.9.1 at 0 and 100% loads. Record transformer surface temperature.

7.3 Replace output transformer (P/N LYP18293D4) with Cubex-iron-core output transformer (P/N LYP18292D1).

7.4 Repeat paragraph 7.2 to determine differences in efficiency.

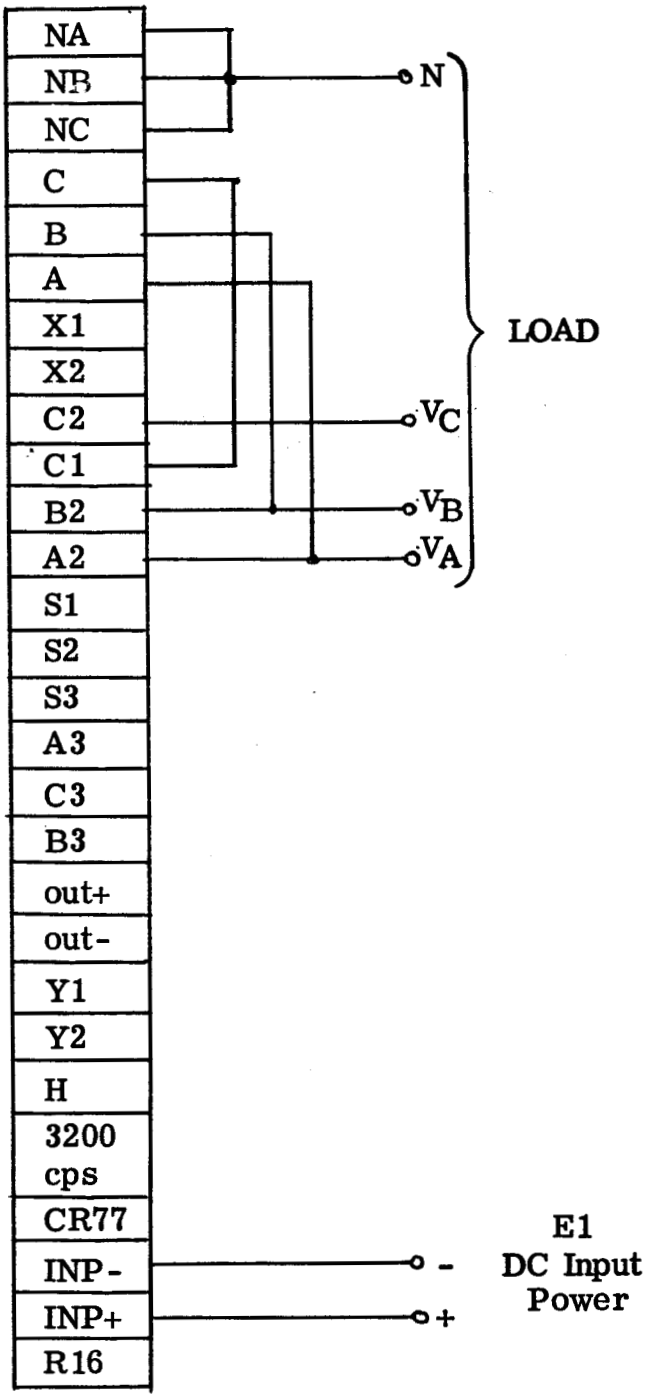

Figure 8. Terminal Connections for Single Inverter Operation and Initial Adjustments. (See Schematic Diagram.)

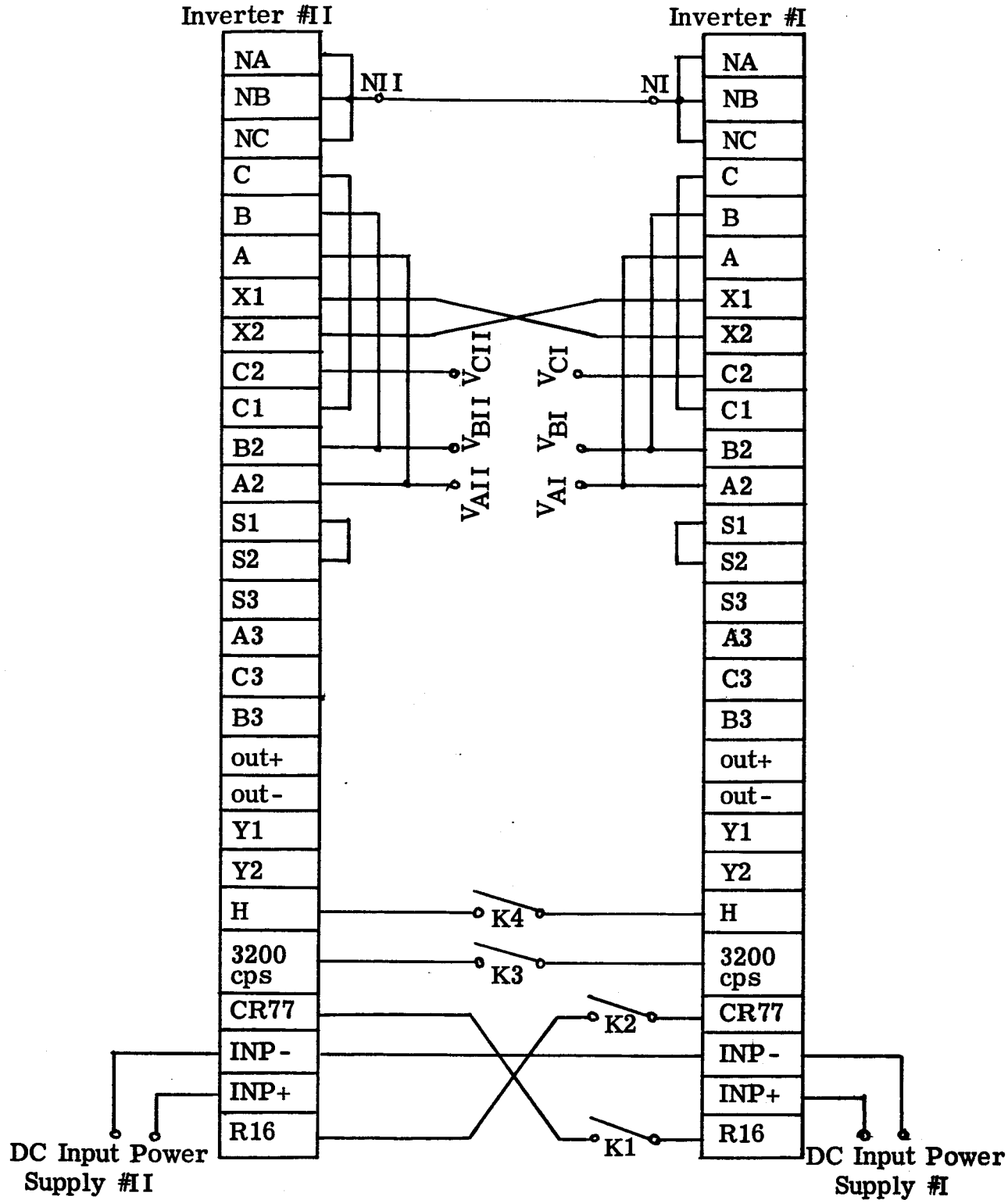

Figure 9. Terminal Connections and Interconnections for Parallel Inverter Operation. (See Schematic Diagram.)

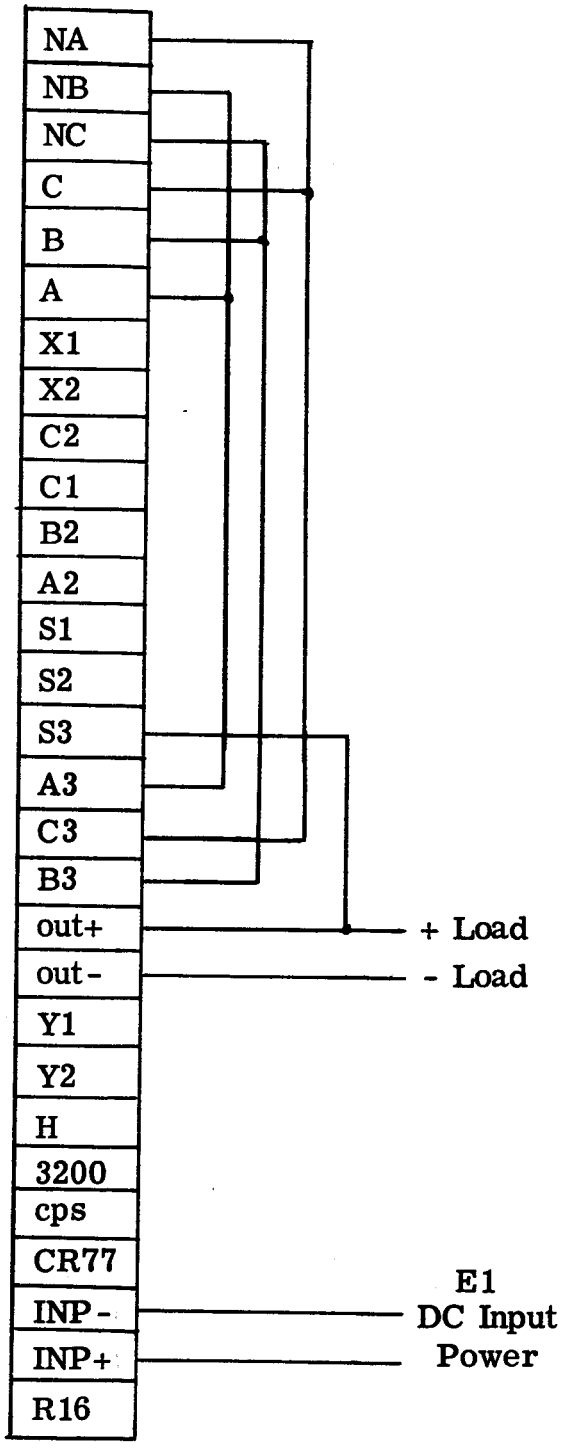

Figure 10. Terminal Connections for Single Converter Operation. (See Schematic Diagram.)

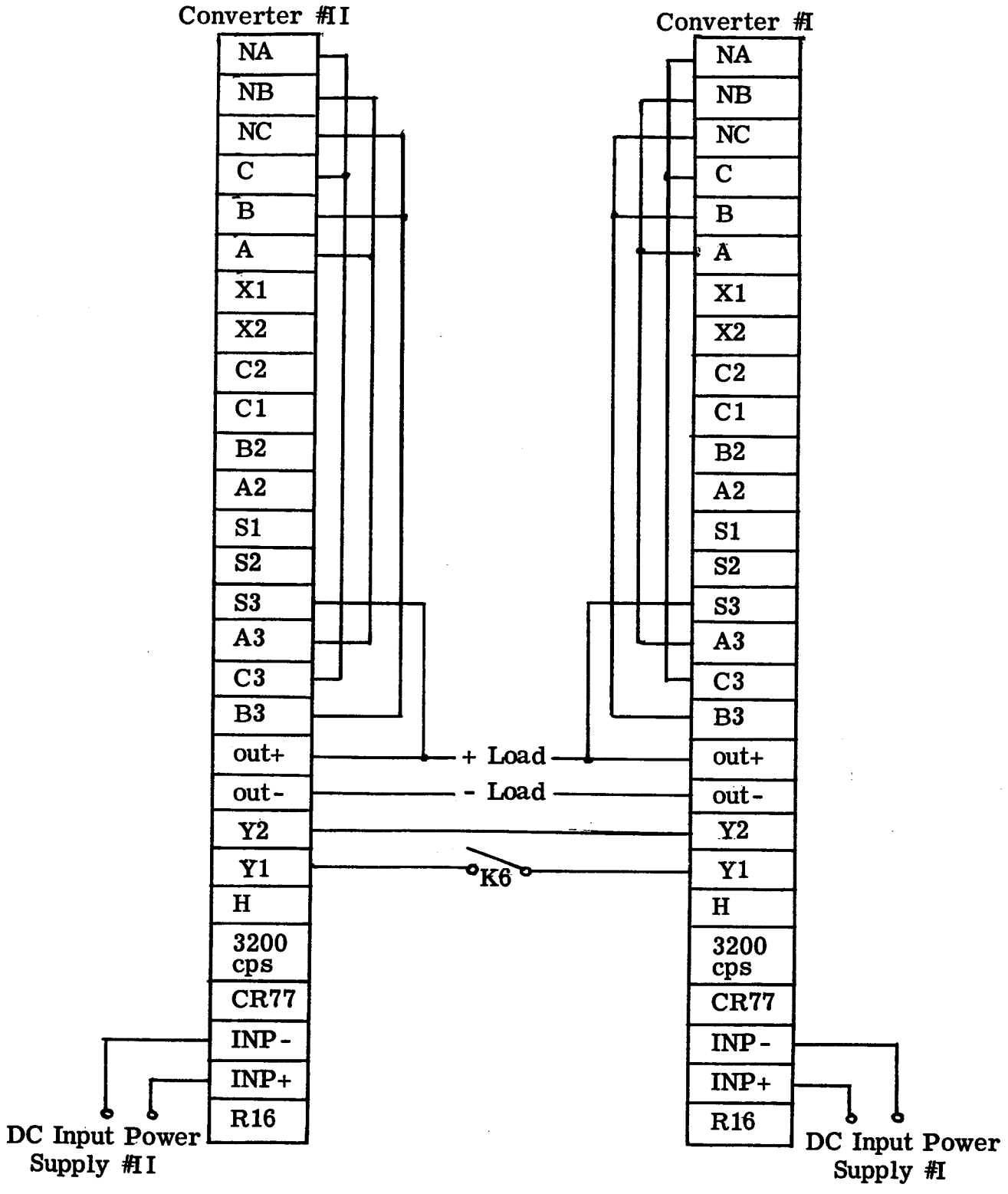

Figure 11. Terminal Connections and Interconnections for Parallel Converter Operation. (See Schematic Diagram.)

DISTRIBUTION LIST

Quarterly and Final Technical Reports

One copy to be sent to each addressee, unless indicated otherwise. Note that more than one addressee may be shown for the same address.

Nationan Aeronautics & Space Administration
Lewis Research Center
21000 Brookpark Road
Cleveland, Ohio (44135)

Attn:	B. Lubarsky MS 86-1	(1)
	R. L. Cummings MS 86-1	(1)
	N. T. Musial MS 77-1	(1)
	J. J. Fackler MS 86-1	(1)
	George Mandal MS 5-5	(3)
	Billy G. Cauley MS 21-4	(1)
	J. P. Quitter MS 4-9	(1)
	C. S. Corcoran, Jr. MS 100-1	(1)
	E. A. Koutnik MS 86-5	(1)
	A. C. Herr MS 77-1	(1)
	F. Gourash MS 86-1	(3)

--*--

National Aeronautics & Space Administration
Goddard Space Flight Center
Greenbelt, Maryland

Attn:	F. C. Yagerhofer	(1)
	H. Carleton	(1)

--*--

National Aeronautics & Space Administration
Marshall Space Flight Center
Huntsville, Alabama

Attn:	James C. Taylor (M-ASTR-R)	(1)
	Richard Boehme (M-ASTR-EC)	(1)

--*--

National Aeronautics & Space Administration
Manned Spacecraft Center
Houston, Texas

Attn:	A. B. Eickmeir (SEDD)	(1)

--*--

National Aeronautics & Space Administration
4th and Maryland Avenue, S.W.
Washington 25, D.C.

Attn: James R. Miles, Sr. (SL) (1)
P. T. Maxwell (RPP) (1)
A. M. Greg Andrus (FC) (1)

--*--

Naval Research Laboratory
Washington 25, D.C.

Attn: B. J. Wilson (Code 5230) (1)

--*--

Bureau of Naval Weapons
Department of the Navy
Washington 25, D.C.

Attn: W. T. Beason (Code RAEE-52) (1)
Milton Knight (Code RAEE-511) (1)

--*--

Jet Propulsion Laboratory
4800 Oak Grove Drive
Pasadena, California

Attn: G. E. Sweetman (1)

--*--

Diamond Ordnance Fuze Laboratories
Connecticut Avenue & Van Ness Street N.W.
Washington, D.C.

Attn: R. B. Goodrich (Branch 940) (1)

--*--

U.S. Army Research & Development Laboratory
Energy Conversion Branch
Fort Monmouth, New Jersey

Attn: H. J. Byrnes (SIGRA/SL-PSP) (1)

--*--

Engineers Research & Development Laboratory
Electrical Power Branch
Fort Belvoir, Virginia

Attn: Ralph E. Hopkins (1)

--*--

DISTRIBUTION LIST (Cont.)

Aeronautical Systems Division
Wright-Patterson Air Force Base
Dayton, Ohio

Attn: Capt. W. E. Dudley - ASRMFP-3 (1)

--*--

University of Pennsylvania
Power Information Center
Moore School Building
200 South 33rd Street
Philadelphia 4, Pennsylvania (1)

--*--

Duke University
College of Engineering
Department of Electrical Engineering
Durham, North Carolina

Attn: T. G. Wilson (1)

--*--

National Aeronautics & Space Administration
Scientific and Technical Information Facility
Box 5700
Bethesda 14, Maryland

Attn: NASA Representative (6 copies + 2 repro.)

--*--

AiResearch Division
Garrett Corporation
Cleveland Office
20545 Center Ridge Road
Cleveland 16, Ohio

Attn: W. K. Thorson (1)

--*--

Westinghouse Electric Corporation
Aerospace Electrical Division
Lima, Ohio

Attn: Andress Kernick (1)

--*--

G. M. Defense Research Lab
General Motors Corporation
Santa Barbara, California

Attn: T. M. Corry (1)

--*--

The Martin Company
Baltimore, Maryland

Attn: Mike Monaco MS 3017 (1)

--*--

General Electric Company
Specialty Control Dept.
Waynesboro, Virginia

Attn: Mr. Lloyd Saunders (1)

--*--

Lear-Siegler, Incorporated
Power Equipment Division
P.O. Box 6719
Cleveland 1, Ohio

Attn: Mr. Robert Saslaw (2)

--*--

The Bendix Corporation
Bendix Systems Division
Ann Arbor, Michigan

Attn: K. A. More (1)

--*--

The Bendix Corporation
Red Bank Division
1900 Hulman Building
Dayton, Ohio

Attn: R. N. Earnshaw (1)

--*--

VARO, Incorporated
2201 Walnut Street
Garland, Texas

Attn: J. H. Jordan (1)

--*--

DISTRIBUTION LIST (Cont.)

Wright-Patterson AFB
AFAPL (APIP-30)
Ohio

Attn: Paul R. Bertheaud (1)

--*--